



Schiff-base appended polymers for phosphate removal

Murat K. Deliomeroğlu, Vincent M. Lynch & Jonathan L. Sessler


To cite this article: Murat K. Deliomeroğlu, Vincent M. Lynch & Jonathan L. Sessler (2017): Schiff-base appended polymers for phosphate removal, *Supramolecular Chemistry*, DOI: [10.1080/10610278.2017.1372581](https://doi.org/10.1080/10610278.2017.1372581)

To link to this article: <http://dx.doi.org/10.1080/10610278.2017.1372581>

 View supplementary material 

 Published online: 05 Sep 2017.

 Submit your article to this journal 

 View related articles 

 View Crossmark data 

Schiff-base appended polymers for phosphate removal

Murat K. Delimeroglu, Vincent M. Lynch and Jonathan L. Sessler 

Department of Chemistry, The University of Texas at Austin, Austin TX, USA

ABSTRACT

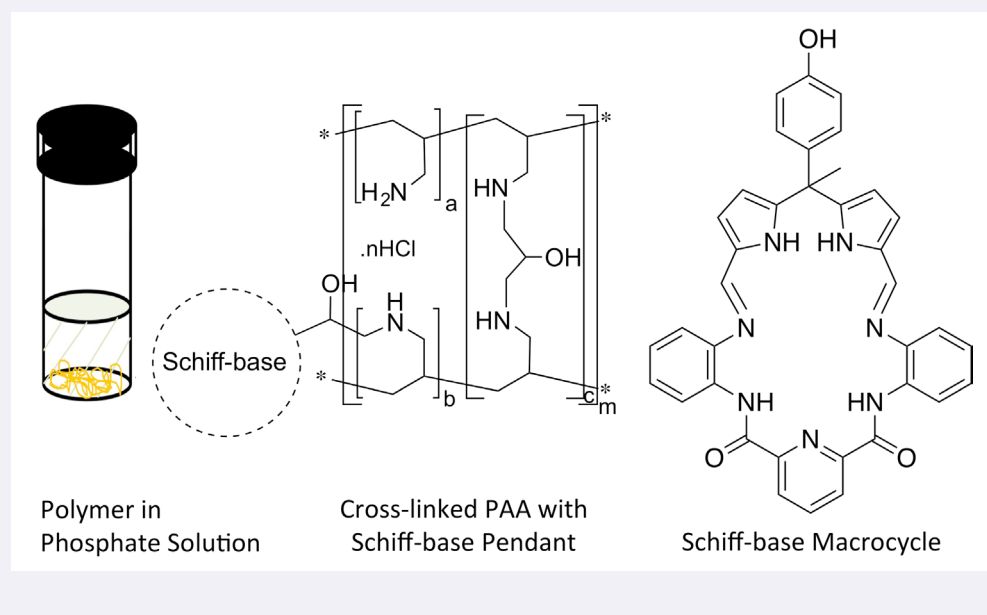
The remediation of phosphate-contaminated water bodies and the effective treatment of hyperphosphatemia are two big challenges in which phosphate recognition could play a useful role. Here, we summarise briefly the state of the art in phosphate removal. Next, we present findings from synthetic and phosphate extraction studies that involve polymeric materials with pendent Schiff-base macrocycles designed to function as phosphate anion receptors.

ARTICLE HISTORY

Received 18 July 2017
Accepted 23 August 2017

KEYWORDS

Anion binding; phosphate; polymers; extraction



Introduction

Some of the challenges associated with anion recognition derive in part from the larger size of anions relative to their isoelectronic cations, the diverse geometries that anions often display, and the higher energies of solvation that must typically be overcome to extract them out of an aqueous phase (1). Anions are generally larger than cations. Therefore, larger hosts are required for recognition of anions (2). The F^- anion, for instance, has an ionic radius of 1.2–1.4 Å (depending on the convention employed) (3). Protonated porphyrins with *trans*-nitrogen distances of about 4 Å and a potential source of four hydrogen bond

donors are too small to bind F^- (4). However, an early solid state structural study of a sapphyrin- F^- complex (Figure 1a) revealed that the F^- ion was bound within the core of this larger pentapyrrolic porphyrin analogue (4). This Sapphyrin has a core size of roughly 5.5 Å (effective diameter) and therefore, possesses a core that is large enough to accommodate a bound F^- anion.

Figure 1 shows two macrocyclic systems, sapphyrin and cyclo[8]pyrrole, each with an anionic guest in its central cavity. In this Figure, the sapphyrin- F^- complex is shown on the left (a), while the cyclo[8]pyrrole- H_2SO_4 salt is shown on the right (b). While a size comparison of differently shaped

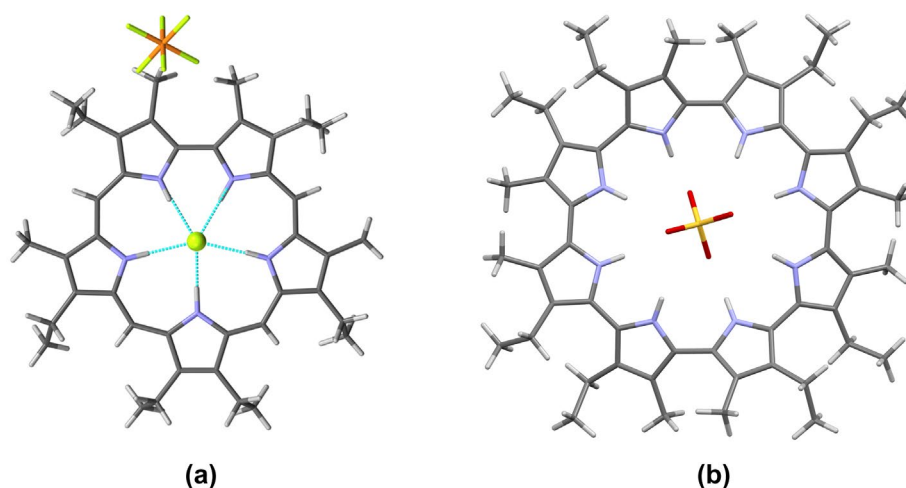


Figure 1. (Colour online) (a) Single crystal structures of the sapphyrin- F^- complex and (b) the cyclo[8]pyrrole- H_2SO_4 salt. These structures were originally reported by Sessler et al. (4),(6) and were redrawn using data from the Cambridge Crystallographic Date Centre (CCDC) as detailed in CCDC numbers 1184078 and 176189, respectively.

anions, such as F^- versus SO_4^{2-} , is necessarily challenging, the tetrahedral sulfate anion, characterised by a sulfur (S) oxygen (O) bond distance of about 1.5 Å (5), is larger than the spherical fluoride anion, at least in a qualitative sense. Consistent with this notion is the finding that the sulfate anion, but not the fluoride anion, is bound well by the diprotonated octapyrrolic macrocycle (Figure 1), which has a relatively large cavity diameter of roughly 7.5–7.7 Å (6).

Inorganic phosphate and its protonated anionic forms (i.e. PO_4^{3-} , HPO_4^{2-} and $H_2PO_4^-$) are, like sulfate, quintessential tetrahedral anions. Their recognition is likely to require not only larger hosts but also appropriately shaped binding sites that favor selective recognition. Consistent with this thinking is the fact that there are more tripodal or cage-like synthetic receptors for phosphate recognition than planar cyclic systems. However, independent of design, cognizance must be taken of the fact that anions of di- and tribasic acids, such as H_3PO_4 and H_2SO_4 , are susceptible to proton transfer (7). The receptor itself can also undergo deprotonation, which can exacerbate issues associated with speciation. This latter issue was elegantly noted by Gale et al., who reported that increasing the acidity of pyrrolic hydrogens within a set of his receptors led to deprotonation by basic anions such as F^- , $H_2PO_4^-$, and benzoate, rather than anion binding (8).

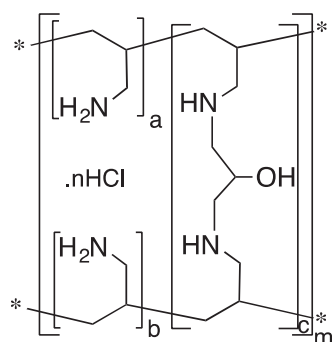
In polar media, including water, anion recognition is rendered further challenging both because of solvation (e.g. $\Delta G_h = -300$ kJ/mol for NO_3^- and $\Delta G_h = -465$ kJ/mol for $H_2PO_4^-$, where ΔG_h = Gibbs free energy change of hydration) (9) and competitive hydrogen bond donation associated with the solvent shell (10). Gabbai and coworkers have been successful in meeting this challenge. They described the synthesis of a cationic Lewis acidic borane which forms a highly stable zwitterionic ammonium/

fluoroborate complex stabilized by a $C-H \cdots F-B$ hydrogen bonds in aqueous media (11). They also demonstrated the use of a cationic borane receptor for the extraction of F^- from water (11). The same group recently employed a neutral bidentate Lewis acid system containing two antimony(V) centers to 'squeeze out' F^- ions from water, thus overcoming the hydration barrier (12). However, to our knowledge, there is no reported artificial receptor capable of extracting $H_2PO_4^-$ out of water into an organic phase. This is true even though the $H_2PO_4^-$ has the same hydration enthalpy value as F^- (9), for which extractants have been reported (13, 14).

Nature has solved the problem of phosphate anion recognition in polar media. Some of the determinants for affecting such biological anion recognition have been inferred from crystallographic studies of the phosphate-binding protein (PBP) from *E. coli* bacteria (15). This periplasmic PBP is involved in the highly selective uptake and active transport of phosphate into bacteria cells and binds its target anion by means of multiple well-oriented hydrogen bonds. It is unlikely that this particular protein will see application in the area of phosphate anion extraction due to its rather high cost.

Nevertheless, biological methods are used in wastewater processing. For instance, the so-called 'enhanced biological phosphate removal' (EBPR) process, involves storage of phosphate as polyphosphates (poly-P) in the form of biomass (16). The underlying mechanism, known as 'luxury uptake', involves circulation of activated sludge through anaerobic and aerobic phases, with the wastewater added during the anaerobic phase (17). By means of the alternating anaerobic-aerobic cycles microorganisms accumulate phosphate in the form of poly-P. Efficient phosphate removal is achieved by the physical removal of the

microorganisms (18) although the underlying microbiology is still far from understood (19). Unfortunately, EBPR is not likely to be applicable to medical applications, such as treating hyperphosphatemia, where biocompatibility is likely to be required.



$$a+b=9, c=1$$

$$n=0.4 \text{ (40\% protonated)}$$

Renigel

Figure 2. Chemical structure of Renigel®.

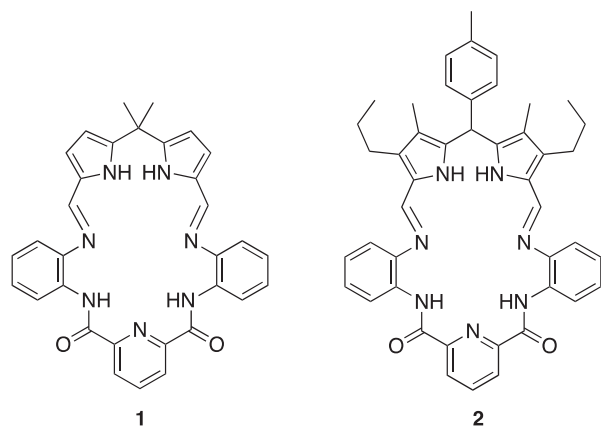


Figure 3. Structures of compounds 1 and 2.

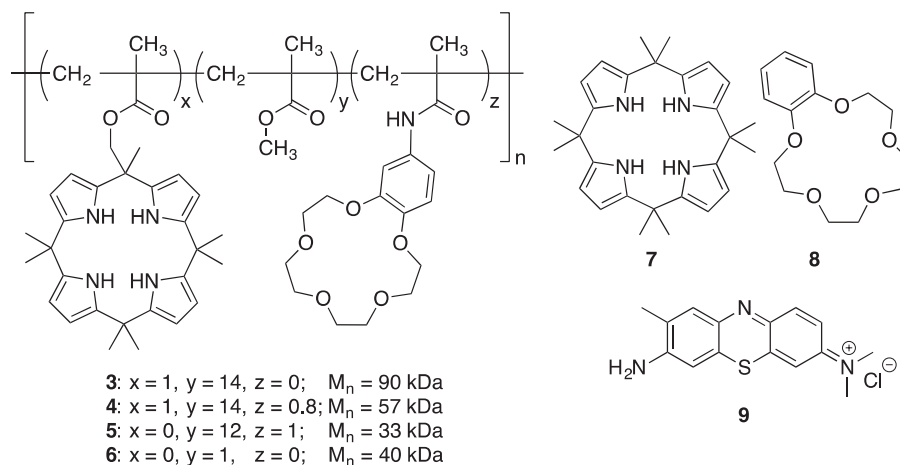


Figure 4. Structures of key compounds from reference (14).

Hyperphosphatemia, or elevated serum phosphate levels, is a disorder that is particularly prevalent among patients with end-stage renal disease (20). The current methods for treating hyperphosphatemia involve various combinations of long (3 h) daily dialysis session, dietary restrictions, consumption of hard cations, or ingestion of Sevelamer (a cross-linked poly(allylamine) (PAA), e.g. Renigel®, *c.f.* Figure 2) (21).

Oral administration of cross-linked PAA serves to control the concentration of phosphorus available for absorption in the gastrointestinal track. This polymer is not selective for phosphate. In fact, it also binds the chloride anion well. Rather high doses must therefore be ingested. Adverse effects are also seen in some patients undergoing Renigel® therapy. We thus believe there remains a need for biologically compatible materials capable of binding phosphate under conditions associated with the treatment of hyperphosphatemia. More broadly, there remains a need for polymers that can serve as extractants for highly hydrated tetrahedral anions. Initial efforts towards attaining these goals are summarised below.

We have previously reported a series of tetrakis(1H-pyrrole-2-carbaldehyde) receptor family, including an electroactive derivative and a hexakis(1H-pyrrole-2-carbaldehyde) derivative as excellent phosphate receptors (22, 23). Two of these macrocyclic Schiff-base structures, compounds 1 and 2 (Figure 3), were chosen as models for the development of polymeric materials containing pendent 2,6-diamidopyridine dipyrromethane (DPM) receptors as detailed further below.

Polymeric materials with pendent phosphate receptors were proposed based on a prior study wherein polymers with pendent calix[4]pyrrole (C[4]P) anion receptors (*c.f.* Figure 4) were used to extract halide anion salts from aqueous phases. In that study, Aydogan and Sessler used a *meso*-functionalized C[4]P system as a pendent receptor on a poly-(methyl methacrylate) (pMMA) backbone to obtain the co-polymer 3 (13). This co-polymer was shown to be

capable of extracting tetrabutylammonium (TBA) chloride (TBACl) and fluoride (TBAF) salts from aqueous media into an CH_2Cl_2 organic phase, under conditions where the control compounds **7** (octamethyl C[4]P) and **6** (a pMMA polymer without the pendant receptors) were not effective.

Aydogan and Sessler improved their first generation C[4]P-pMMA material (**3**) by creating a co-polymer (**4**) that also contained a pendent cation-binding receptor (benzo-15-crown-5, **8**) (**14**). Co-polymer **4**, which contains both pendent anion and cation receptors, was found capable of extracting halide salts from water as ion-pairs, namely KF and KCl, into an organic phase. The anion extraction could be followed visually by using a cationic dye with a Cl^- counter anion (**9**). This colored reagent was carried from the aqueous solution into the organic phase (CH_2Cl_2) by the polymer **4**, as inferred from the observed color changes. This was not true for any control systems, including monomer **7**, crown ether **8**, the monofunctionalized polymer **3**, pMMA **6** or combinations thereof (**14**). The extraction events were also monitored by various analytical methods, e.g. ^1H and ^{19}F NMR spectroscopy and flame emission spectroscopy. Against this background an effort was made to functionalize the known phosphate anion receptors **1** and **2** such that they could be incorporated into polymers.

Experimental

Synthesis

(4E,13E)-2-(4-Methoxyphenyl)-2-methyl-1¹H,3¹H-5,7,11,13-tetraaza-9(2,6)-pyridina-1,3(2,5)-dipyrrola-6,12(1,2)-dibenzenacyclotetradecaphane-4,13-diene-8,10-dione (21)

In a 50 ml round bottom flask, **14** (46.4 mg, 0.144 mmol, 1 equiv.) and **20** (50 mg, 0.144 mmol) were dissolved in dry methanol (20 ml). Concentrated H_2SO_4 (16.9 μL , 0.317 mmol, 2.2 equiv.) was then added using a syringe. The resulting solution was heated at reflux under argon for 15 min. The volatiles were removed under reduced pressure. The residue obtained in this way was washed with CHCl_3 to give a salt-like orange-brown solid. This crystalline solid was redissolved in CH_3OH . An excess of triethylamine (TEA; 0.1 ml) was added to this solution. The resulting mixture was heated at reflux for 15 min then was cooled to room temperature. The product was collected in the form of a light pink precipitate, which was washed with cold methanol to yield the free-base macrocycle. ^1H NMR (500 MHz, CD_2Cl_2) δ 9.52 (bs, 2H), 8.27 (d, 2H, $J = 7.8$ Hz), 8.23 (s, 2H), 8.02 (t, 1H, $J = 7.9$ Hz), 7.59 (dd, 2H, $J = 7.8$ Hz, $J = 1.7$ Hz), 7.24 (dt, 2H, $J = 7.4$ Hz, $J = 1.6$ Hz), 7.20 (dt, 2H, $J = 7.4$ Hz, $J = 1.6$ Hz), 7.11 (dd, 2H, $J = 7.8$ Hz, $J = 1.7$ Hz), 6.82 (d, 2H, $J = 8.8$ Hz), 6.74 (d, 2H, $J = 3.8$ Hz), 6.65 (d, 2H, $J = 8.8$ Hz), 6.33 (d, 2H, $J = 3.8$ Hz), 3.67 (s, 3H), 2.01 (s, 3H) ppm. ^{13}C NMR (126 MHz, CD_2Cl_2) δ

164.0, 159.1, 151.6, 150.4, 146.2, 143.7, 139.4, 138.7, 131.3, 131.0, 128.6, 127.7, 127.2, 126.4, 126.0, 119.6, 119.4, 114.3, 109.7, 55.7, 45.4, 29.5 ppm. HRMS (ESI+) m/z for $\text{C}_{38}\text{H}_{32}\text{N}_7\text{O}_3$ $[\text{M}]^+$ calcd 634.25565, found 634.25611.

(4E,13E)-2-(4-Hydroxyphenyl)-2-methyl-11H,31H-5,7,11,13-tetraaza-9(2,6)-pyridina-1,3(2,5)-dipyrrola-6,12(1,2)-dibenzenacyclotetradecaphane-4,13-diene-8,10-dione (22)

The procedure reported for the formation of the other Schiff-base macrocycle **21** was followed, albeit with **15** and **20** as the starting materials. In a 100 ml round bottom flask, compound **15** (352 mg, 1.1 mmol) and compound **20** (347 mg, 0.98 mmol) were dissolved in distilled methanol (60 ml). H_2SO_4 conc. (115 μL , 2.1 mmol) was then added dropwise using a syringe. The resulting solution was heated at reflux under argon for 15 min. The solution was cooled to room temperature and an excess of TEA was added via syringe. The solution was stirred at room temperature for 15 min. The product was collected in the form of a very pale yellow precipitate and washed with cold methanol to yield 490 mg of macrocycle **22** (93% yield). ^1H NMR (400 MHz, $\text{DMSO}-d_6$) δ 10.99 (bs, 2H), 10.33 (s, 2H), 9.26 (s, 1H), 8.14–8.16 (m, 3H), 8.05 (s, 2H), 7.35 (d, 2H), 7.26 (t, 2H), 7.16 (t, 2H), 7.04 (d, 2H), 6.57–6.59 (m, 6H), 6.12 (d, 2H), 1.88 (s, 3H) ppm. ^{13}C NMR (150 MHz, $\text{DMSO}-d_6$) δ 163.2, 155.8, 151.5, 149.2, 149.0, 142.8, 139.3, 137.7, 130.7, 129.4, 128.1, 127.6, 127.3, 124.9, 124.4, 119.8, 117.3, 114.7, 108.7, 44.2, 29.7 ppm. HRMS (ESI+) m/z for $\text{C}_{37}\text{H}_{29}\text{N}_7\text{O}_3$ $[\text{M} + \text{H}]^+$ calcd 620.24063, found 620.24046.

Co-polymer 24

To a solution of **22** (340 mg, 0.55 mmol) in DMF (5 mL), were added Cs_2CO_3 (185 mg, 0.56 mmol) and CsBr (2 mg). The resultant mixture was stirred for 15 min at room temperature. A solution of the chloromethyl functionalized polymer **23** (85 mg, containing *c.a.* 0.55 mmol Cl atom) was then added. The mixture was heated to 80 $^\circ\text{C}$ for 12 h. The reaction mixture was then allowed to cool to room temperature. Before being sparged into CH_3OH , the insoluble precipitates were removed by filtration. The filtrate was precipitated in CH_3OH (200 mL). The precipitate that resulted was filtered and dried *in vacuo*. The solid obtained was dissolved in CH_2Cl_2 and insoluble inorganics and non-reacted **22** were removed by filtration. CH_2Cl_2 was removed under reduced pressure. Compound **24** was solidified with CH_3OH and dried *in vacuo* to give a light yellow powder (210 mg).

Compound 27

A similar procedure used to obtain co-polymer **24** was employed, albeit with compounds **22** and **30** as starting materials. The product (**27**) proved stable enough to characterise but not to store on the bench top. ^1H NMR

(400 MHz, CDCl_3) δ 9.51 (bs, 2H), 8.23 (d, $J=7.8$ Hz, 2H), 8.19 (s, 2H), 7.91 (t, $J=7.8$ Hz, 1H), 7.59 (dt, $J=7.2$ Hz, $J=2.0$ Hz, 2H), 7.17 (m, 4H), 7.04 (dd, $J=7.2$ Hz, $J=2.0$ Hz, 2H), 6.80 (d, $J=8.9$ Hz, 2H), 6.68 (d, $J=3.7$ Hz, 2H), 6.63 (d, $J=8.8$ Hz, 2H), 6.29 (d, $J=3.7$ Hz, 2H), 4.08 (dd, $J=11.0$ Hz, $J=3.0$ Hz, 1H), 3.76 (dd, $J=11.0$ Hz, $J=5.8$ Hz, 1H), 3.22 (m, 1H), 2.81 (t, $J=4.9$ Hz, 1H), 2.64 (dd, $J=4.9$ Hz, $J=2.7$ Hz, 1H), 2.0 (s, 3H) ppm. ^{13}C NMR (101 MHz, CDCl_3) δ 163.5, 157.2, 150.7, 149.7, 149.7, 142.7, 138.9, 138.6, 130.6, 128.1, 127.1, 126.5, 125.9, 125.6, 125.6, 118.8, 118.6, 114.4, 109.2, 68.7, 50.0, 36.5, 31.3, 29.3 ppm. HRMS (ESI⁺) calcd for $\text{C}_{40}\text{H}_{33}\text{N}_7\text{O}_4$ [$\text{M} + \text{H}$]⁺ 676.26670, found 676.26750.

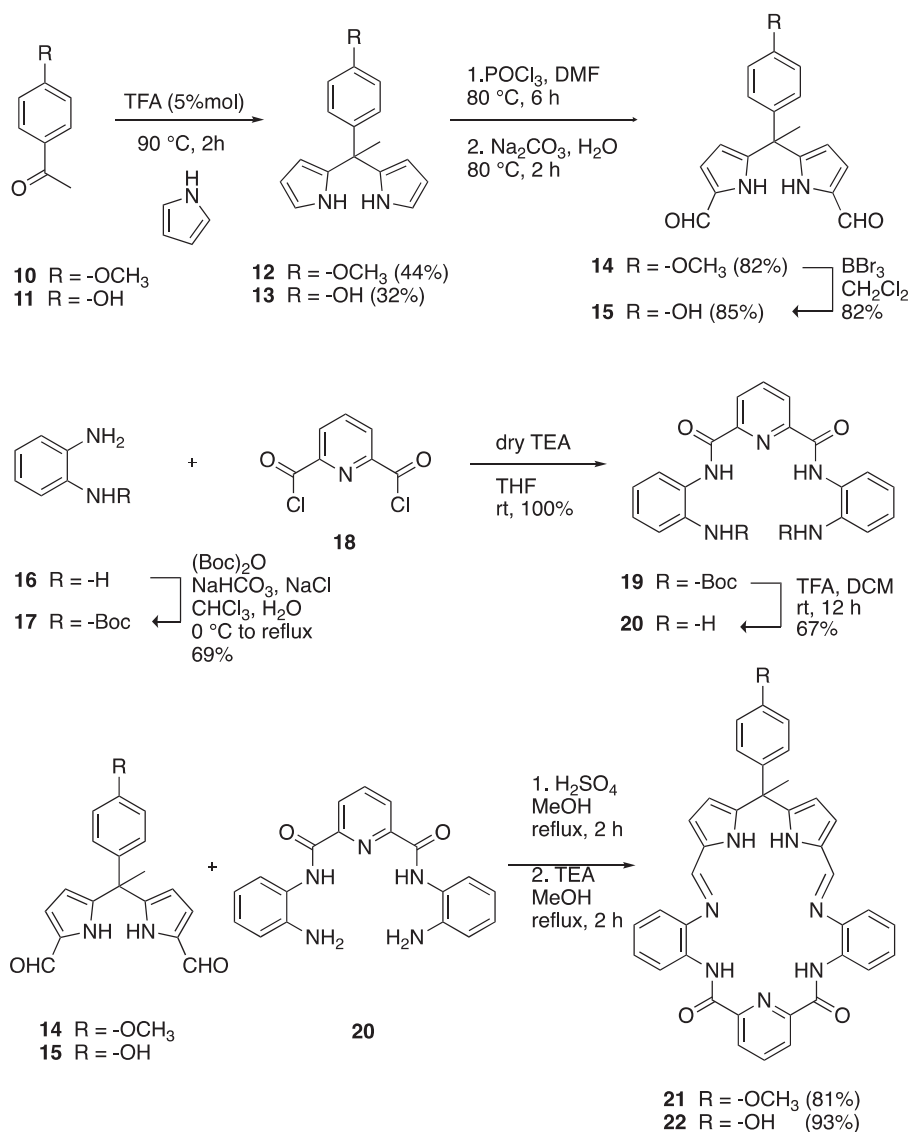
Randomly cross-linked PAA-HCl (32) and the randomly cross-linked PAA-HCl derivative with Schiff-base pendants (33)

A 20% w/v solution of PAA-HCl (160 mg, 0.8 ml) was mixed with a 10 M solution of NaOH (68 mg) until the exotherm

subsided. The reaction vessel was then allowed to cool down to room temperature. At this point, the reaction mixture was split into two equal parts. To one portion, the cross-linker (EPI, **30**) (40 mg) was added. To the other one, precursor **27** (49 mg) along with EPI (**30**) (40 mg) was added. Both mixtures formed gels within an hour. The dried gel slabs, corresponding to **32** and **33**, were ground into small pieces for use in solid-liquid extraction studies.

Results and discussion

Two new Schiff-base macrocycles, **21** and **22**, were constructed by cyclisation of the dialdehydes **14** and **15** with diamine **20** via diimine formation (Scheme 1). The dialdehydes **14** and **15** and the diamine **20** were prepared according to literature procedures (24, 26). All structures were characterised by ^1H and ^{13}C NMR spectroscopy and high-resolution mass spectrometry (HRMS). ^1H NMR



Scheme 1. Synthesis of Schiff-base macrocycles **21** and **22**.

spectroscopy was used to monitor the formation of imine bonds in the final step. Imine bond formation was confirmed by the absence of a signal at 9.4 ppm (the resonance frequency for the aldehyde CH proton of **15**) and the presence of a signal at 8.3 ppm ascribed to the imine CH proton (*cf.* Figure 5). Figure 6 shows the X-ray crystal structures of two precursors **15** and **20** and the two Schiff-base macrocycles **21** and **22**.

While macrocycle **21** was designed as a control compound, macrocycle **22** was designed to serve as a precursor that would allow attachment of the Schiff-base macrocyclic framework to a polymeric support. In other words, it was expected that macrocycle **22** would allow access to polymeric materials with pendent Schiff-base receptors.

Solid state structural studies were carried out using single crystals of **21** co-crystallized with CH₃OH and **22** co-crystallized with DMF. Both structures revealed similar conformations in which the aryl moiety of the DPM subunit (originating from **15**) and the pyridine moiety (originating from **20**) are in *cis* positions relative to the *o*-phenylene rings. Based on the conformational similarity between the single crystal structures of **21** and **22**, it was inferred that the methyl group did not have a substantial impact

on the conformation of the macrocyclic framework. This lack of difference was considered to augur well for the use of macrocycles functionalized in the phenolic position as precursors for polymer formation.

It is also instructive to compare the conformations of these two new Schiff-base macrocycles (**21** and **22**) with those of similar macrocycles reported previously, namely **1** (**24**) and **2** (**26**). Reported modeling studies showed that the free ligands **1** and **2** could exist in two different conformations (**26**). In the case of **2**, the tolyl and pyridine fragments were calculated to adopt either in *trans* or *cis* positions relative to the *o*-phenylene rings. However, single crystal structures of both **21** and **22** revealed a *cis*-like conformation. The contrast was thought to arise from two structural differences in the DPM subunits. Compound **2** has a tolyl ring, a hydrogen atom, and two fully β -substituted pyrrole rings in the *meso*-position, whereas the new system **22** has an aryl ring, a methyl group, and two β -free pyrrole rings.

It is likely that these structural differences, particularly those involving the *meso*-positions and the β -substituents of the pyrrole rings, are reflected in the actual conformations observed for macrocycles **1**, **2**, **21**, and **22**.

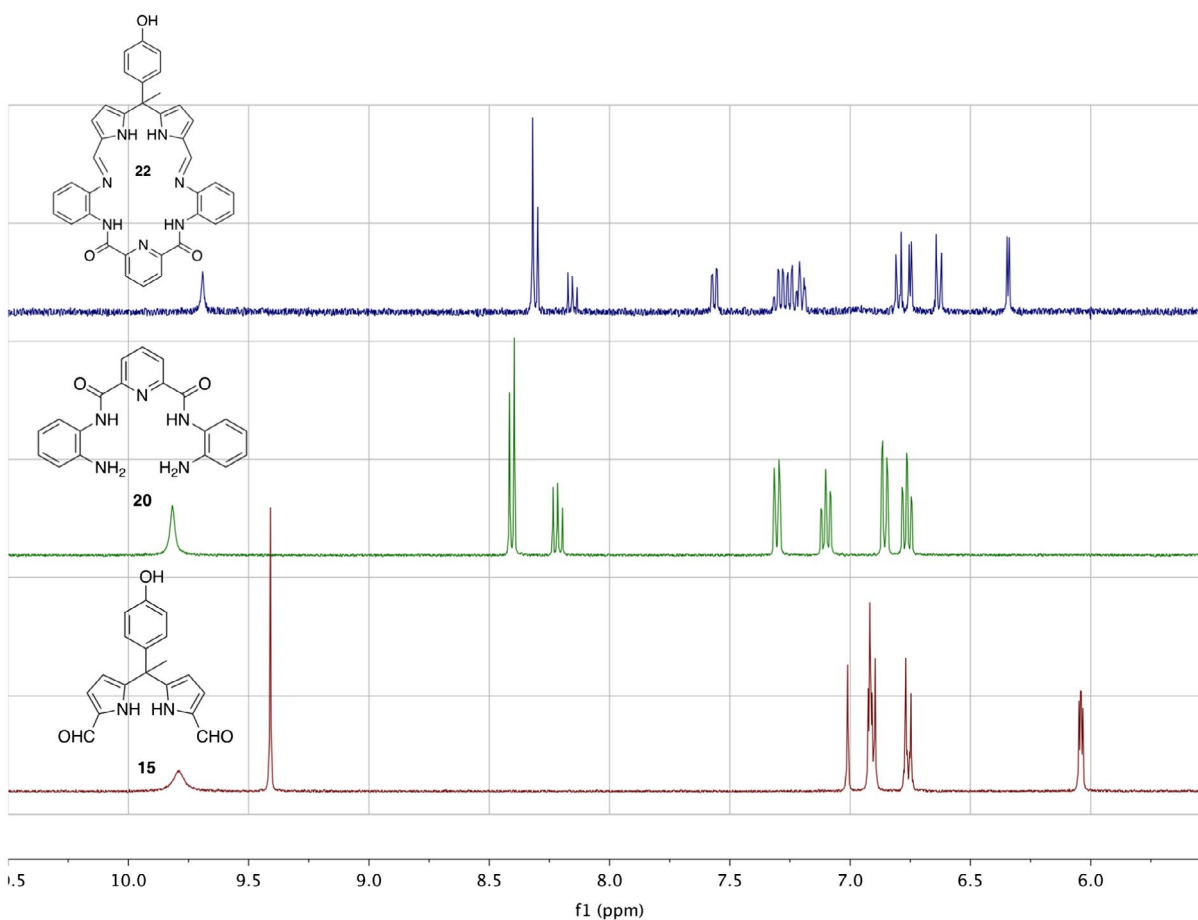


Figure 5. (Colour online) Stacked partial ¹H NMR spectra of **15** (bottom), **20** (middle), and **22** (top) in CD₃CN.

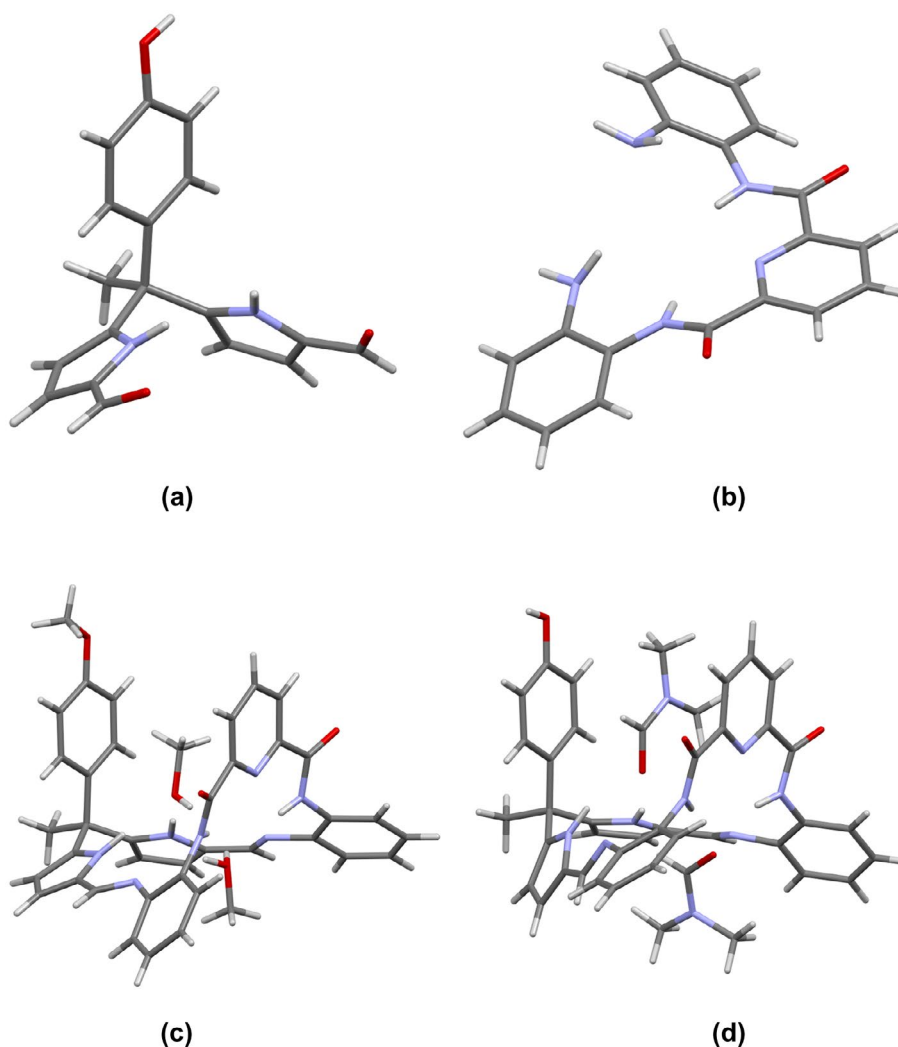


Figure 6. (Colour online) Single crystal structures of (a) **15**, (b) **20**, (c) **21**·2CH₃OH, and (d) **22**·2DMF.

Anion binding studies of **21** and **22**

It was considered possible that the anion binding affinities of the new receptor systems could differ from one another and related prior systems because of these inferred structural differences. The anion binding affinities of the new systems, **21** and **22**, were thus tested.

Figure 7 shows partial ¹H NMR spectra of **21** recorded in CD₂Cl₂ in the presence of varying molar equivalents of TBAH₂PO₄. Major changes in the chemical shifts of the pyrrole NH signals and the imine CH signals are observed (cf. Figure 7). Saturation behavior of the changes in the shifts is observed after approximately 2.5 M equivalents of TBAH₂PO₄ had been added to the initial receptor solutions.

For quantification of the binding affinities, UV-vis spectroscopic studies, in which receptor **21** was titrated with TBAH₂PO₄ and TBAHSO₄ in CH₂Cl₂, were conducted. Experimental details and spectra are presented in the Supplemental Material. Table 1 shows the binding affinities

obtained from the titration studies, as well as the affinities previously reported for **1** (**24**) and **2** (**26**) in CH₃CN.

From the binding affinity constants listed in Table 1, the order of anion selectivity of **21** for the oxyanions H₂PO₄⁻ and HSO₄⁻ in CH₂Cl₂ is the same as that of the receptor **1** in CH₃CN. However, the H₂PO₄⁻ binding stoichiometries of the two systems (**21** and **1**) differ. A 1:2 binding stoichiometry for H₂PO₄⁻ was reported for **1**. Formation of **1**·2H₂PO₄⁻ complex was supported by a competition study in which a solution of **1** containing 10 M equivalents of HSO₄⁻ was titrated with H₂PO₄⁻ (**24**). The spectral changes observed in the case of **1** were interpreted in terms of the receptor having a second binding site for H₂PO₄⁻ that was effective for dihydrogen phosphate anion complexation even in the presence of 10 M equivalents of HSO₄⁻ (**24**).

Receptor **21**, on the other hand, displayed a 1:1 binding stoichiometry for H₂PO₄⁻ anion in CH₂Cl₂. The isosbestic point observed¹ at 327 nm in the UV-vis spectral titration is most easily interpreted in terms of two absorbing species at

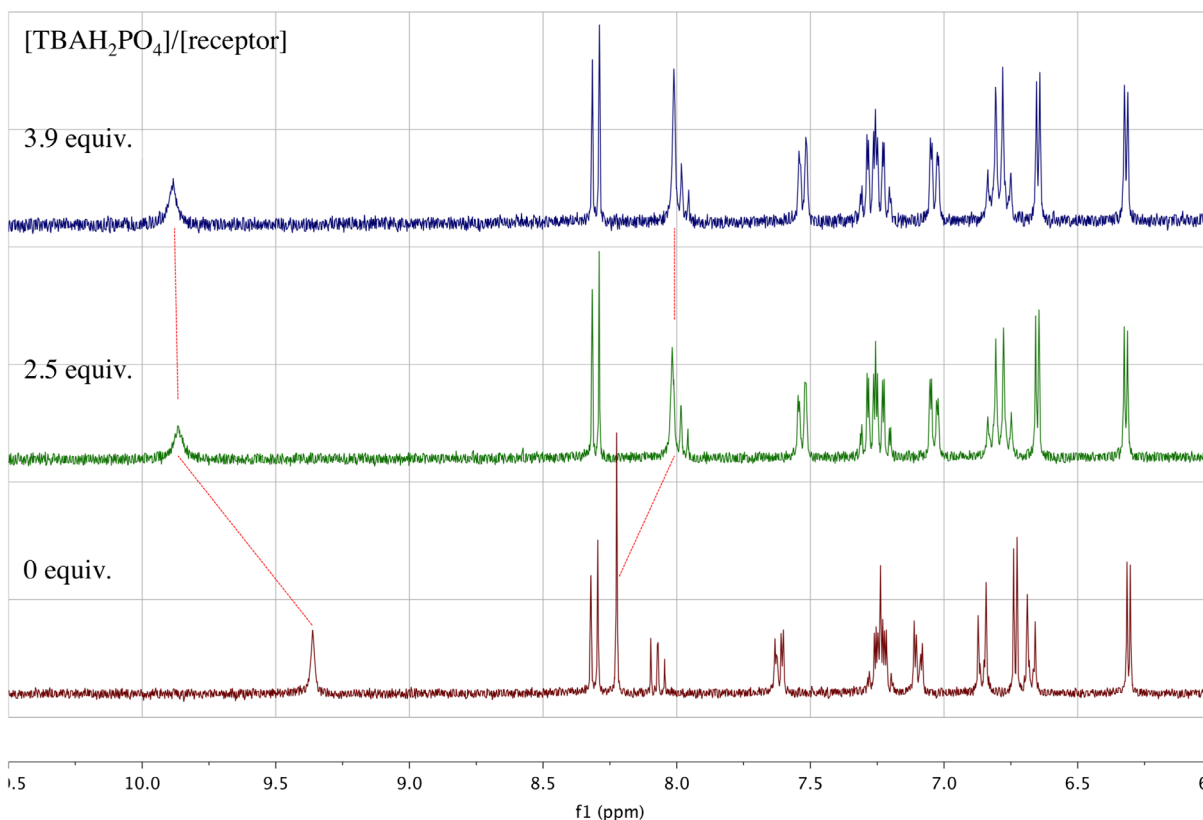


Figure 7. (Colour online) Stacked partial ^1H NMR spectra of **21** in CD_2Cl_2 at varying molar ratio of TBAH_2PO_4 .

Table 1. Binding affinity constants (in M^{-1}) for **21**, **22**, **1**, and **2** with TBA^+ salts of oxyanions as determined by UV-vis spectroscopy in the specified solvents.

Anion	21 ^a	22 ^b	1 ^{b,c}	2 ^{b,d}
H_2PO_4^-	$(2.1 \pm 0.3) \times 10^5$	1.7×10^5	$K_1 = 3.4 \times 10^5$ $K_2 = 2.6 \times 10^4$	$(2.9 \pm 0.2) \times 10^4$
HSO_4^-	$(1.2 \pm 0.2) \times 10^4$	nd	$(6.4 \pm 0.3) \times 10^4$	$(1.1 \pm 0.2) \times 10^5$

^aIn CH_2Cl_2 .

^bIn CH_3CN .

^cReported in reference-(24).

^dIn reported in reference-(26), nd: not determined.

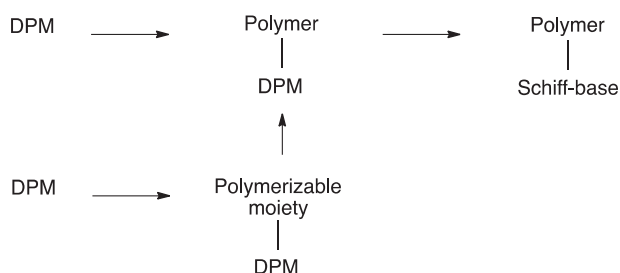
this wavelength (namely, the free receptor **21** and the bound form of the receptor, $\text{21}\cdot\text{H}_2\text{PO}_4^-$) that are interconverting between one another. A Job plot obtained from the same experiment likewise proved a 1:1 binding stoichiometry. Additionally, the data obtained from UV-vis spectra could be fit well to a 1:1 binding isotherm. Based on these observations, we conclude that receptor **21** has high affinity and selectivity for the H_2PO_4^- anion and binds this target with a 1:1 binding stoichiometry in organic media (i.e. CH_2Cl_2).

Among the receptors listed in Table 1, macrocycle **2** displays the greatest affinity for HSO_4^- . This was rationalised in terms of its ‘frozen’ conformation, which presumably results from the fact that the β -positions of the pyrrole units are substituted and that a sterically restricting tolyl group is present on one of the ‘*meso*-like’ positions of the DPM subunit.

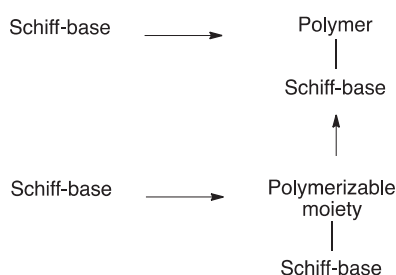
One of the most substantial differences between the two new receptors, **21** and **22**, was their relative solubilities. In fact, derivative **22**, the putative precursor for polymeric materials, displayed low solubility in organic solvents (e.g. CH_2Cl_2 , CHCl_3 , CH_3OH , and CH_3CN), whereas **21** was freely soluble at the mM level in typical halogenated solvents. The low solubility of **22** precluded quantitative analyses in CH_2Cl_2 . It could be studied in CH_3CN , the same solvent in which **1** and **2** were studied. The affinity constant of **22** for H_2PO_4^- was determined ($K_a = 1.7 \times 10^5 \text{ M}^{-1}$ via UV-vis spectroscopy and $K_a = 1.6 \times 10^5 \text{ M}^{-1}$ via ITC) and proved competitive with those of previous receptors. Although it was intended that structure **22** would be further modified at the phenolic position to allow its development as a polymer precursor, it was gratifying that the core macrocycle proved effective for H_2PO_4^- binding.

Synthesis of polymeric material with pendent schiff-base macrocycles

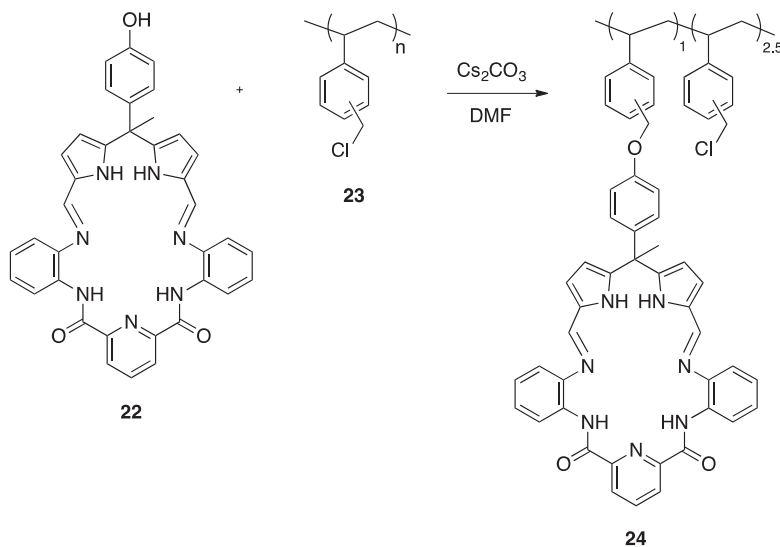
In order to obtain polymeric materials containing pendent Schiff-base macrocycles, two general synthetic approaches were considered. The first approach involved attachment of DPM subunits to a polymer backbone



Scheme 2. First synthetic approach considered for the synthesis of polymeric materials containing Schiff-base macrocyclic pendants. It starts from diuopyromethane precursors.



Scheme 3. Second synthetic approach considered for the synthesis of polymeric materials containing Schiff-base macrocyclic pendants. This approach relies on the use of precursors containing the preformed macrocycle.



Scheme 4. Preparation of polymer **24** by means of post-polymerisation modification of the commercially available functionalized polystyrene **23** with **22**.

(or to a polymerizable moiety) before formation of the Schiff-base macrocycle (Scheme 2). The second approach involved attachment of pre-formed Schiff-base systems (e.g. **22**) to a polymer backbone (or to a polymerizable moiety) (Scheme 3).

The approach involving the attachment of a preformed functionalized Schiff-base to a functionalized polymer backbone was tested first. The functionalized Schiff-base **22**, prepared in 93% yield (see Experimental Section), was attached to the commercially available functionalized-polystyrene **23** (poly(vinylbenzyl chloride), 60:40 mixture of the 3- and 4- isomers) under S_N2 reaction conditions (Scheme 4).

As inferred from integration of the ¹H NMR spectrum (the ratio of the signal at 9.5 ppm to those at 9–5.5 ppm), the new polymeric material **24** bears one pendent Schiff-base macrocycle for approximately every 3.5 phenyl groups present on the styrene backbone (*cf.* Figure 8). In other words, the reaction between equimolar amounts of **22** and **23** yielded about 30% substitution of **23** with **22**. The net result is a co-polymer, **24**, bearing pendent Schiff-base macrocycles (Scheme 4). Co-polymer **24** proved appreciably soluble in CHCl₃. It could thus be used for liquid-liquid and solid-liquid extraction studies as detailed below.

Anion binding studies of co-polymer 24 in CHCl₃ via UV-vis spectroscopy

UV-vis spectroscopy was used to confirm the presence of the pendent Schiff-base macrocycles in the case of co-polymer **24**. Polymer **23**, lacking absorbance features in the 300–400 nm spectral range, reacted with compound **22**,

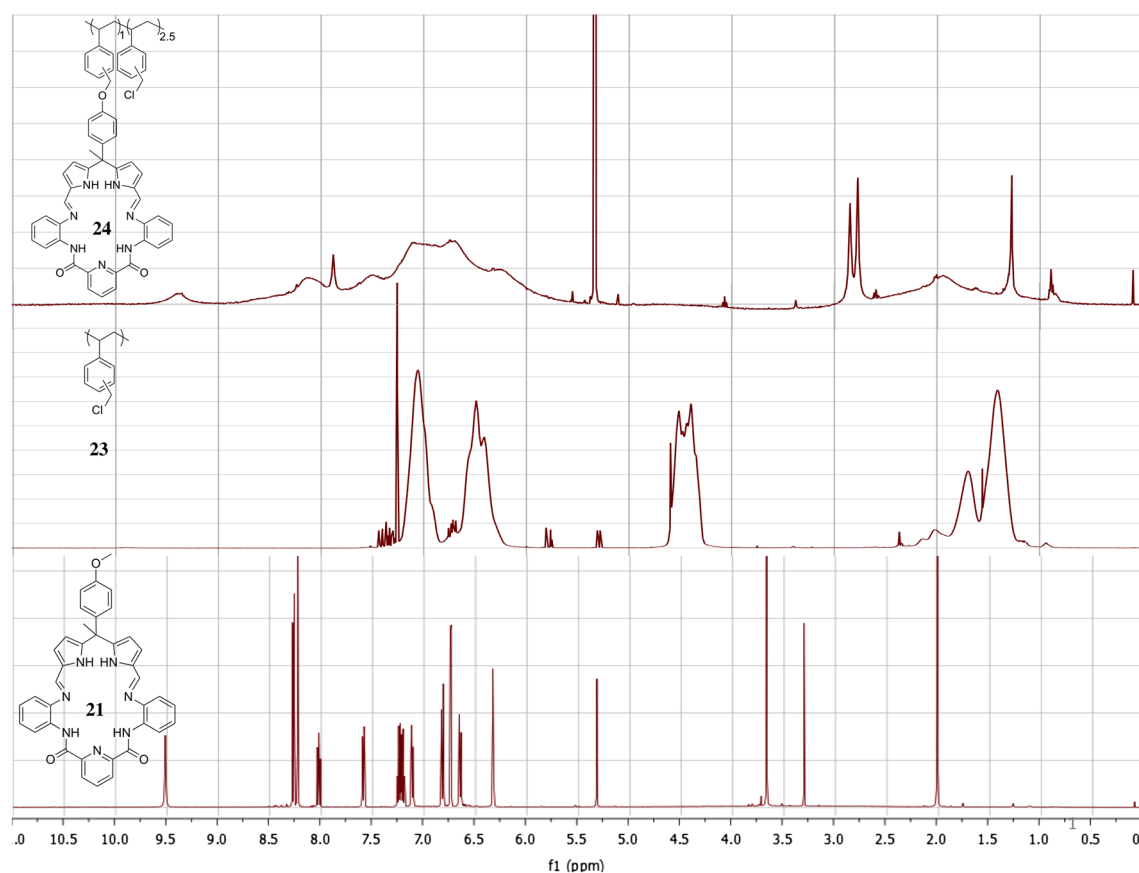


Figure 8. (Colour online) ^1H NMR spectra of **21** in CD_2Cl_2 (bottom), commercially available functionalized polystyrene **23** in CDCl_3 (middle), and co-polymer product **24** in CD_2Cl_2 (top).

which is insoluble in CHCl_3 . The product, assumed to be co-polymer **24**, proved soluble in CHCl_3 . Moreover, it displayed UV-vis spectral features between 300 and 400 nm in CHCl_3 that are characteristic of a Schiff-base macrocycle such as **22** (cf. Figure 9(a)).

Solutions of **24** in CHCl_3 were screened for spectral changes when treated with various TBA^+ anion salts. Among the halide anions, F^- induced the biggest spectral change (Figure 9(b)). The spectrum of **24** that resulted upon exposure to TBAH_2PO_4 was similar to those produced when **21** was treated with H_2PO_4^- (cf. Figure 9c and Figure S.5). On the other hand, the addition of TBAHSO_4 addition caused a spectral change in **24** that differed from what was observed when **21** was exposed to the same salt (Figure 9(c)). The effect of TFA on the spectrum of **24** in CHCl_3 was also tested. The spectral change (Figure 9(d)) was attributed to protonation of the two imine groups present in the Schiff-base macrocycle framework.

Extraction studies with co-polymer **24**

Copolymer **24** was tested for its ability to extract H_2PO_4^- anion salts using two experimental techniques. The first

involved a liquid-liquid extraction. In this case, a solution of co-polymer **24** in CDCl_3 was layered with a solution of TBAH_2PO_4 in D_2O (Figure 10). After shaking² and separating the phases, changes in the H_2PO_4^- anion concentration in both phases were quantified via ^{31}P NMR spectroscopy using either phenylphosphonic acid (PhPO_3H) (in D_2O) or TBAF_6 (in CDCl_3) as the internal standards.

The second method involved solid-liquid extraction studies. Here, solid co-polymer **24** was added into a solution of TBAH_2PO_4 in CD_3OD (or in D_2O in a separate experiment). After shaking and separating off the solution phase, the change in the H_2PO_4^- anion concentration in CD_3OD was quantified via ^{31}P NMR spectroscopy using PhPO_3H as the internal standard. The results are summarised in Table 2. These results proved hard to interpret. The common result among four entries was an increase in the concentration of H_2PO_4^- in the source phase (i.e. stock H_2PO_4^- solution that was tested for extraction). Although removal of H_2PO_4^- from its original source phase was the desired outcome, the unexpected increase in H_2PO_4^- concentration in the source phase can be explained by the removal of water from the H_2PO_4^- source phase, leading to a more concentrated H_2PO_4^- solution.

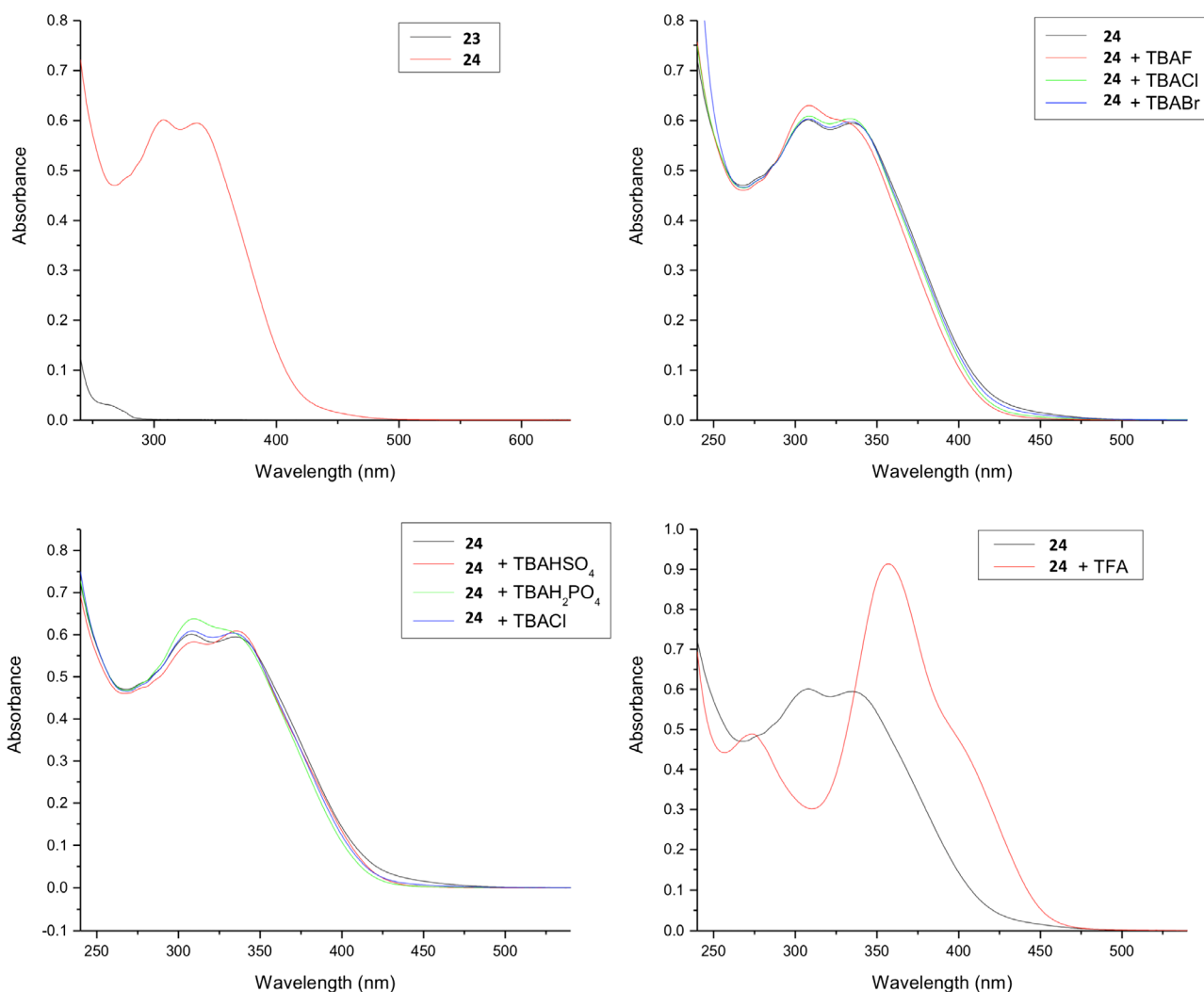


Figure 9. (Colour online) UV-vis spectra in CHCl_3 of (a) the polymer **23** (7.5 mg/L) and co-polymer **24** (18.6 mg/L), (b) **24** in the presence of various TBA^+ halide salts, (c) **24** in the presence of various TBA^+ anion salts, (d) addition of TFA into a solution of **24**.

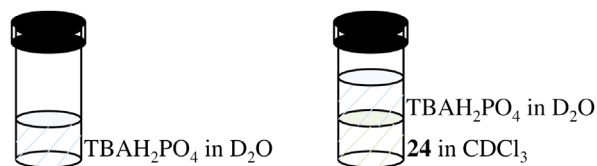


Figure 10. (Colour online) Graphical presentation of the liquid-liquid extraction approach used to test co-polymer **24** as a possible phosphate anion extractant (using TBA^+ as the anion source). Left: H_2PO_4^- solution in D_2O , Right: Biphasic mixture obtained by adding a solution of co-polymer **24** in CDCl_3 to the solution on the left.

Figure 11 shows the UV-vis spectra of **24** in CHCl_3 before exposing to water, after shaking with water, and after shaking with an aqueous TBAH_2PO_4 solution. The major spectral difference was the change observed in the relative

Table 2. Results of extraction studies conducted with co-polymer **24** as a putative extractant.

Extraction type	Source solvent	Extractant solvent	% Change ($[\text{H}_2\text{PO}_4^-]$)	
	$[\text{H}_2\text{PO}_4^-]^a$, V	[24] , V	In source	In extractant
Liquid-liquid	D_2O	CDCl_3		
	50 mM, 1.0 mL	10 mg/1.0 mL	+13%	0%
Solid-liquid	CD_3OD	Solid 24		
	20 mM, 1.5 mL	10 mg	-6%	-
	50 mM, 1.5 mL	10 mg	+4%	-
Solid-liquid	D_2O	Solid 24		
	50 mM, 1.0 mL	11 mg	+6%	-

^a TBAH_2PO_4 was used as the H_2PO_4^- source. V stands for volume. % Changes were quantified by using internal standard (PhPO_3H or TBAPF_6) via ^{31}P NMR spectroscopy.

intensity of the two maxima of the co-polymer **24** after contacting with water. This was seen independent of the H_2PO_4^- content in the source phase.

During the liquid-liquid extraction study conducted with **24**, gelation behavior was seen regardless of the content of the aqueous solutions. On the basis of this observed gelation behavior and the UV-vis spectral changes seen when **24** (in CHCl_3) is brought into contact with an aqueous phase, we propose that this polymeric material can absorb water. Removing water from the aqueous phase under conditions of liquid-liquid would serve to increase the effective TBAH_2PO_4 concentration in the source phase, thus accounting for the results in Table 2.

Synthesis of cross-linked polymeric material with pendent schiff-base macrocycles

Since the attachment of **22** to **23** to obtain co-polymer **24** using substitution chemistry (*vide supra*) worked well, various other modifications in the phenolic position of **22** were tested. Macrocycle **22** was substituted regioselectively in

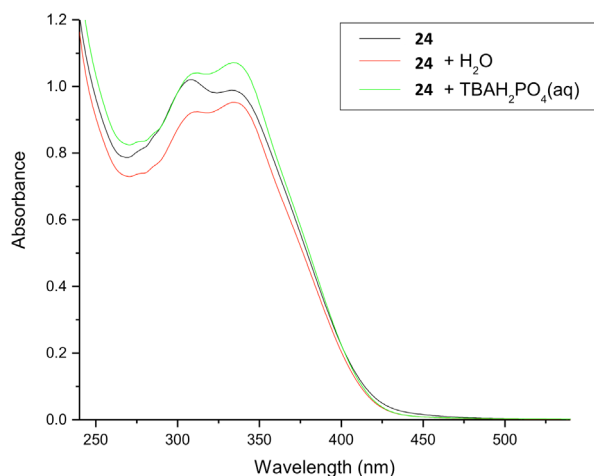


Figure 11. (Colour online) UV-vis spectra of **24** (25 mg/L) in CHCl_3 (black), **24** in CHCl_3 after vigorous shaking with deionized (DI) water (red), and **24** in CHCl_3 after shaking with aqueous TBAH_2PO_4 solution (green).

its phenolic position with a polymerizable styrene unit, a clickable propargyl group, and a cross-linker, epichlorohydrin (EPI). This gave compounds **25**, **26**, and **27**, respectively (Scheme 5).

In order to incorporate the new macrocyclic framework into a cross-linked PAA network, the synthetic route shown in Scheme 6 was followed. The control system (**32**), an EPI (**30**) cross-linked PAA, was prepared along with a pendent Schiff-base containing derivative, **33**. Both hydrogels were prepared via an aqueous reaction of a 20% w/v solution of linear PAA-HCl chains and EPI, which served as the crosslinking agent (**27**). The commercially available PAA-HCl (Alfa Aesar) used in the synthesis of the gels had molecular weights of 120,000–200,000 g/mol. Before crosslinking, the polymer chains, some of the HCl groups of PAA-HCl were neutralised by adding NaOH solution. This provides free NH_2 sites for the subsequent EPI cross-linking reaction. For the synthesis of **33**, Schiff-base **27** was added along with EPI in the cross-linking step. Two insoluble systems, **32** and **33**, resulted. Both were tested as possible H_2PO_4^- extractants using a solid-liquid extraction approach.

Extraction studies with **33**

Figure 13 shows three ^{31}P NMR spectra arising from the solid-liquid extraction studies in which **32** and **33** were used in conjunction with KH_2PO_4 . The bottom spectrum is of a stock KH_2PO_4 solution (46 mM) in D_2O containing phenylphosphonic acid (PhPO_3H , 33 mM) as the internal standard.

The spectrum in the middle is of the KH_2PO_4 (1.0 mL) aliquot after it had been treated with control cross-linked PAA **32** (15 mg). A decrease in H_2PO_4^- concentration from 46 to 35 mM was observed. The top spectrum is of a separate KH_2PO_4 (1.0 mL) aliquot after having been treated with Schiff-base appended cross-linked PAA **33** (15 mg). A decrease in H_2PO_4^- concentration from 46 mM

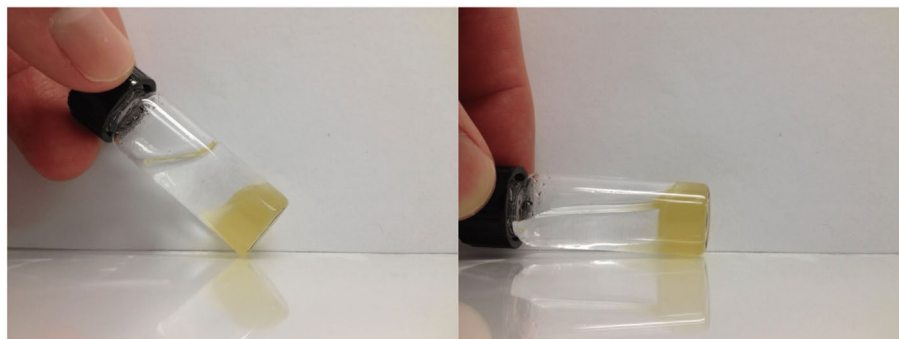
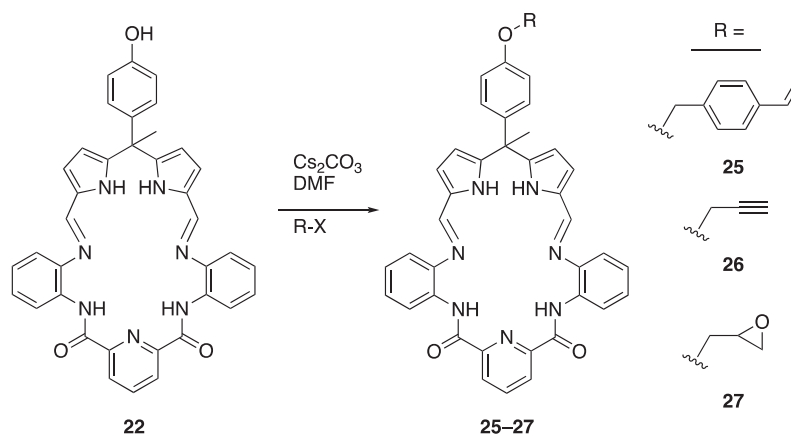
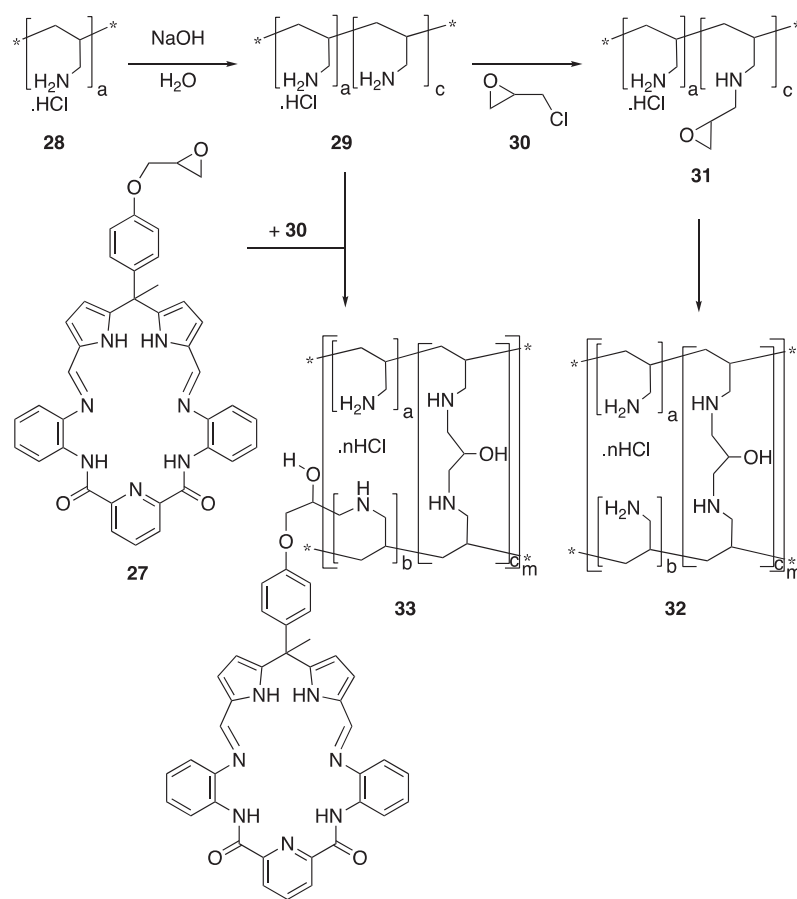


Figure 12. (Colour online) Photos of gel formed during the extraction study with the co-polymer **24**. The bottom layer initially consisted of a solution of the co-polymer **24** in CHCl_3 while the top layer was an aqueous anionic salt solution.



Scheme 5. Syntheses of **25–27** via nucleophilic substitution.



Scheme 6. Synthetic route used to prepare a cross-linked polymeric material with pendant Schiff-base macrocycles (**33**). Also shown is a synthesis of a control system without the pendant macrocycles (**32**).

to 38 mM was observed. On this basis, it was concluded that the functionalized solid hydrogel **33** (15 mg) was no more effective at extracting H_2PO_4^- than the same amount of solid hydrogel **32**, after accounting for differences in effective molecular weights. On this basis, we conclude that electrostatic effects override any putative

benefit associated with attaching a receptor to the polymer system. While disappointing, this result serves to underscore the need for more effective receptor design in the construction of polymeric materials designed to promote the extraction of anionic salts into organic media.

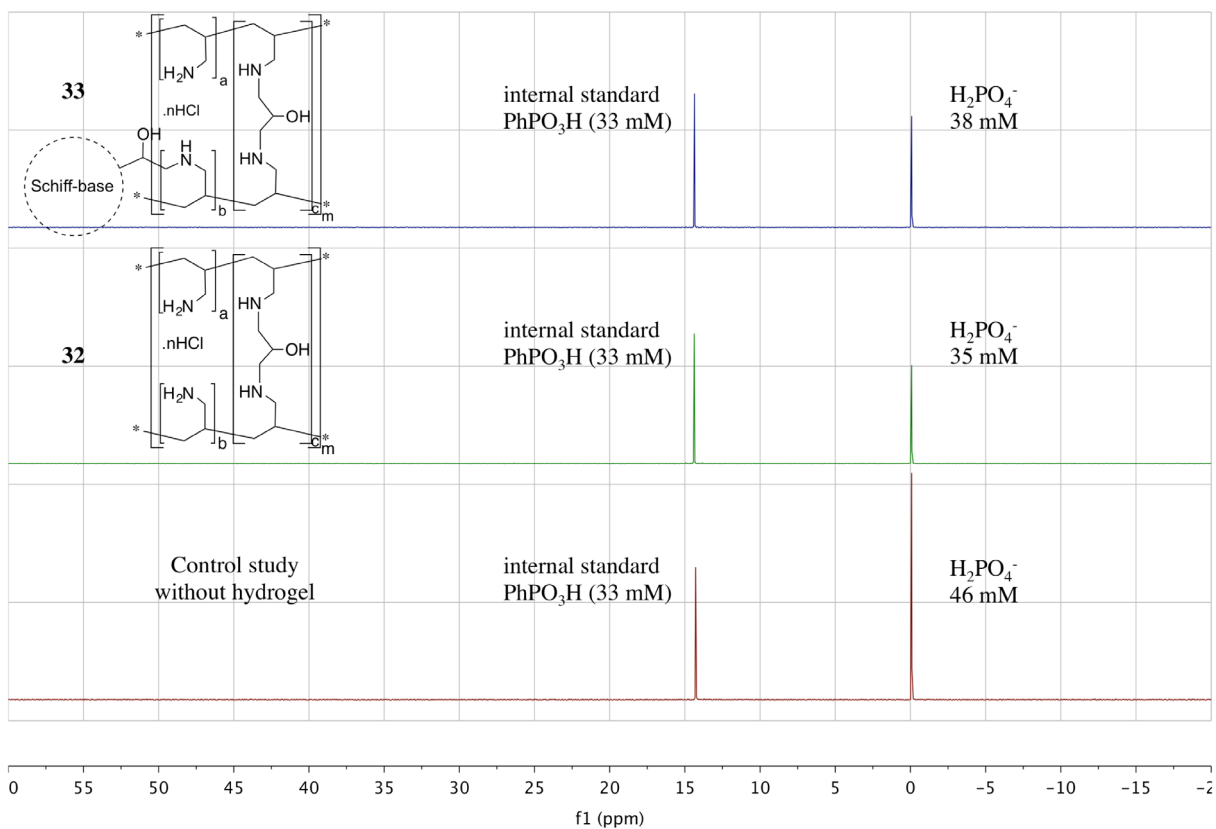


Figure 13. (Colour online) Stacked partial ^{31}P NMR spectra (recorded in D_2O) of a stock KH_2PO_4 solution (46 mM) containing phenylphosphonic acid (PhPO_3H , 33 mM) as the internal standard (bottom), the stock aqueous KH_2PO_4 solution (1.0 mL) after treatment with cross-linked PAA **32** (15 mg) containing PhPO_3H (33 mM) as the internal standard (middle), and the stock aqueous KH_2PO_4 solution (1.0 mL) after treatment with the Schiff-base appended cross-linked PAA **33** (15 mg) containing PhPO_3H (33 mM) as the internal standard (top).

Conclusion

A new functionalized Schiff-base macrocyclic framework, which relies on a formylated-DPM as a precursor, was prepared. Control compound **21**, bearing this new framework, was studied for its anion binding properties in CH_2Cl_2 . It was concluded that **21** displays higher affinity for H_2PO_4^- than it does for HSO_4^- in CH_2Cl_2 . In this solvent, the H_2PO_4^- anion is bound with a binding stoichiometry 1:1 (**21**: H_2PO_4^-). Covalent attachment of the new framework to a polymeric backbone was achieved using derivative **22**. It was shown that **22** could be attached to many different systems via substitutions involving the phenolic position of **22**. In this way, derivatives **25–27** were prepared. The co-polymer **24**, also obtained via a substitution reaction, was studied for its anion binding potential in CHCl_3 via UV-vis spectroscopy and for its extraction ability. Little change in the feature of co-polymer **24** was seen in CHCl_3 with all anions tested, including the common halides, H_2PO_4^- , and HSO_4^- (all as their TBA^+ salts). Under conditions of liquid-liquid extraction, co-polymer **24** forms gels, independent of whether an anion is present in the aqueous phase. Extraction studies did not reveal a reduction in the H_2PO_4^- concentration

in the source aqueous solution when **24** was tested as an extractant.

A hydrogel containing pendent Schiff-base macrocycles (**33**) was also prepared. In hydrogel **33**, pendent Schiff-bases were covalently attached to a PAA backbone by adding a mixture of **27** and EPI during the cross-linking step. Solid-liquid extraction studies revealed that **33** is able to extract KH_2PO_4 into an organic phase, but is not efficient in doing so than a control hydrogel **32**, a result that is rationalised in terms of non-specific electrostatic interactions dominating over receptor-based binding in the case of the present systems. Current work is focused on preparing polymers bearing functionality designed to enhance anion and ion pair recognition.

Notes

1. The total concentration of the receptor species was held constant throughout the titration of **21** with TBAH_2PO_4 .
2. Shaking a biphasic mixture co-polymer **24** in CDCl_3 and TBAH_2PO_4 in D_2O causes gelation. Gelation occurs in the bottom layer (i.e. CDCl_3). A photo of the resulting gel is shown in Figure 12.

Disclosure statement

No potential conflict of interest was reported by the authors.

Funding

This work was supported by the U.S. Department of Energy, Office of Basic Energy Sciences [grant number DE-FG02-01ER15186 to J.L.S.].

ORCID

Jonathan L. Sessler  <http://orcid.org/0000-0002-9576-1325>

References

- (1) Sessler, J.L.; Gale, P.A.; Cho, W.-S. *Anion Receptor Chemistry*; The Royal Society of Chemistry: Cambridge, UK, 2006.
- (2) Steed, J.W.; Turner, D.R.; Wallace, K. *Core Concepts in Supramolecular Chemistry and Nanochemistry*; Wiley, Hoboken, NJ, 2007.
- (3) Rashin, A.; Honig, B. *J. Phys. Chem.* **1985**, *89*, 5588–5593.
- (4) Sessler, J.L.; Cyr, M.J.; Lynch, V.; McGhee, E.; Ibers, J.A. *J. Am. Chem. Soc.* **1990**, *112*, 2810–2813.
- (5) Katayev, E.A.; Boev, N.V.; Khrustalev, V.N.; Ustynyuk, Y.A.; Tananaev, I.G.; Sessler, J.L. *J. Org. Chem.* **2007**, *72*, 2886–2896.
- (6) Seidel, D.; Lynch, V.; Sessler, J.L. *Angew. Chem. Int. Ed.* **2002**, *41*, 1422–1425.
- (7) Jeffrey, G.A. *An Introduction to Hydrogen Bonding (Topics in Physical Chemistry)*; Oxford University Press, 1997.
- (8) Camiolo, S.; Gale, P.A.; Hursthouse, M.B.; Light, M.E.; Shi, A.J. *Chem. Commun.* **2002**, *3*, 758–759.
- (9) Marcus, Y.J. *J. Chem. Soc., Faraday Trans* **1991**, *87*, 2995–2999.
- (10) Schmidtchen, F.P.; Berger, M. *Chem. Rev.* **1997**, *97*, 1609–1646.
- (11) Chiu, C.W.; Gabbai, F.P. *J. Am. Chem. Soc.* **2006**, *128*, 14248–14249.
- (12) Hirai, M.; Gabbai, F.P. *Angew. Chem. Int. Ed.* **2015**, *54*, 1205–1209.
- (13) Aydogan, A.; Coady, D.J.; Lynch, V.M.; Akar, A.; Marquez, M.; Bielawski, C.W.; Sessler, J.L. *Chem. Commun.* **2008**, 1455–1457.
- (14) Aydogan, A.; Coady, D.J.; Kim, S.K.; Akar, A.; Bielawski, C.W.; Marquez, M.; Sessler, J.L. *Angew. Chem. Int. Ed.* **2008**, *47*, 9648–9652.
- (15) Wang, Z.; Luecke, H.; Yao, N.; Quiocho, F.A. *Nat. Struct. Biol.* **1997**, *4*, 519–522.
- (16) Levin, G.V.; Shapiro, J. *Water Environ. Fed.* **1965**, *37*, 800–821.
- (17) Barnard, J.L. *Water Res.* **1975**, *9*, 485–490.
- (18) Mino, T.; van Loosdrecht, M.C.M.; Heijnen, J.J. *Water Res.* **1998**, *32*, 3193–3207.
- (19) Mino, T. *Biochemistry. (Mosc.)* **2000**, *65*, 341–348.
- (20) Goldsmith, D.R.; Scott, L.J.; Cvetković, R.S.; Plosker, G.L.; Bihl, G.; Kidney, W.; West, S.; Africa, S.; Bommer, J. *Drugs* **2008**, *68*, 85–104.
- (21) Ayus, J.C.; Achinger, S.G.; Mizani, M.R.; Chertow, G.M.; Furmaga, W.; Lee, S.; Rodriguez, F. *Kidney Int.* **2007**, *71*, 336–342.
- (22) Deliomeroglu, M.; Lynch, V.; Sessler, J. *Chem. Commun.* **2014**, *50*, 11863–11866.
- (23) Deliomeroglu, M.; Lynch, V.; Sessler, J. *Chem. Sci.* **2016**, *7*, 3843–3850.
- (24) Sessler, J.L.; Katayev, E.; Pantos, G.D.; Ustynyuk, Y.A. *Chem. Commun.* **2004**, 1276–1277.
- (25) Lee, C.H.; Na, H.K.; Yoon, D.W.; Won, D.H.; Cho, W.S.; Lynch, V.M.; Shevchuk, S.V.; Sessler, J.L. *J. Am. Chem. Soc.* **2003**, *125*, 7301–7306.
- (26) Sessler, J.L.; Katayev, E.; Pantos, G.; Scherbakov, P.; Reshetova, M.D.; Khrustalev, V.N.; Lynch, V.M.; Ustynyuk, Y.A. *J. Am. Chem. Soc.* **2005**, *127*, 11442–11446.
- (27) Kioussis, D.R.; Smith, D.F.; Kofinas, P. *J. Appl. Polym. Sci.* **2001**, *80*, 2073–2083.
- (28) Lee, C.-H.; Lindsey, J.S. *Tetrahedron* **1994**, *50*, 11427–11440.
- (29) Varghese, S.; Senanayake, T.; Murray-Stewart, T.; Doering, K.; Fraser, A.; Casero, R.A.; Woster, P.M. *J. Med. Chem.* **2008**, *51*, 2447–2456.